Angewandte Chemie
Eine Zeitschrift der Gesellschaft Deutscher Chemiker

Supporting Information

69451 Weinheim, Germany

Measurement of amyloid fibril length distributions by inclusion of rotational motion in solution-state NMR diffusion measurements[**]

*Andrew J Baldwin, Spencer J Anthony-Cahill, Tuomas PJ Knowles, Guy Lippens, John Christodoulou, Paul D Barker, Christopher M Dobson**

Supplementary Information

S1 - Methodology

Materials

$Apo-(SH3)_2Cytb_{562}$ was expressed and purified from *E.coli* as described elsewhere[1]. Fibrils were formed at low pH and purified by ultracentrifugation at 290k g for 1 hour in a Beckman-Coulter TLA-120 rotor, such that 10S and larger species were sedimented. The pellet fraction was resuspended in 3 mM HCl and the cycle repeated to ensure smaller monomeric and oligomeric protein has been removed.

NMR

NMR data were acquired on Bruker Avance500 and 700 instruments equipped with cryoprobes. Sample concentrations varied between 20 and 100 μM protein, calculated in terms of total number of monomeric units. The sample analysed in particular detail (figure 2 of the main manuscript) was at a concentration of 60μM. The spectra of individual samples were unchanged when recorded at different times over periods of weeks. Re-purification of a previously purified fibril samples by ultracentrifugation, showed only trace material (<1%) in the second supernatant, demonstrating that the monomer/fibril exchange timescale is much slower than the timescale of the experiment.

The pulsed field gradient stimulated echo (PFGSE) sequence with 3-9-19 water suppression (Bruker pulse sequence *stebpgp1s19*) was used for the diffusion experiments with p30=2.7ms (hence δ=2$\times$p30=5.4ms). The diffusion delay, Δ was varied as described in the manuscript. Corrections for sample viscosity were made by simultaneously measuring the self-diffusion of water. For a 'conventional' diffusion experiment, d20 was set to 100ms. Processing of FIDs was performed using NMRPipe[2], performed in batch using scripts written using c shell. Numerical analysis of the raw NMR data and subsequent fitting to the diffusion model were performed using in-house software programmed in C++, making use of the GNU Scientific Library (GSL)[3], with outputs visualised using Gnuplot, via scripts generated by the program. Source code is available on request.

The intensity profiles shown were obtained by integrating signal intensities of high S/N peaks in the spectrum. By comparing the variation of measured decay constants between individual recorded frequencies one can estimate experimental uncertainties. Estimating the uncertainty in this way gives comparable results to the uncertainties obtained from repeating experiments to calculate the standard error.

TEM

Bright field TEM images were taken on a Philips CM100 transmission microscope operating at 80kV. Contrast between sample and substrate was achieved with uranyl acetate negative staining. Typically 25 p moles of fibril were added to UV irradiated formvar and carbon coated 400 mesh nickel grids. The fibrils were sufficiently spaced so that length distributions could be determined using ImageJ[4].

AFM

AFM data were acquired using a Molecular Imaging Pico Plus microscope operating in AC-AM mode (tapping mode) in air. Ultrasharp Micromasch NCS36 silicon cantilevers were used at resonance frequency of 150 kHz. Typically 25pm of fibrils in 20 μl were deposited onto a freshly cleaved mica surface. The samples were then left to dry in air for 60 min whilst shielded from dust particles. Images were analysed with ImageJ[4] to determine length distributions.

S2 - The Einstein-Stokes equation

Rotational D_R and translational D_T diffusion coefficients are given by $D = \frac{kT}{f}$, where f is an appropriate friction factor, k is the Boltzman constant and T is temperature. For small hard spheres, the translational friction factor is given by Stokes' law as $6\pi\eta R_H$, where η is the viscosity of the solution and R_H is the hydrodynamic radius of the sphere. The Einstein-Stokes equation is therefore:

$$D_T^{sphere} = \frac{kT}{6\pi\eta R_H} \tag{1}$$

Diffusion coefficients obtained from PFGSE measurements can be directly related to the geometry of species under study via the friction factors. In the data shown shown in figure 1D, the NMR diffusion coefficients were calculated for each recorded frequency over a range of peaks using the ST equation. These were converted into R_H estimates using the Einstein-Stokes equation, allowing a histogram to be constructed. Analysis of the histogram allowed a mean value and experimental uncertainty estimate to be determined from the FWHM the histogram, as shown in Figure 1D. Diffusion measurements from 10 independent fibril preparations are shown in figures 1C and D in the primary manuscript.

S3 - Relationship between rotational and translational displacements

The microscopic motions of particles due to translation and rotation are related through the mean squared displacement $< z^2 >$ for translational diffusion D_T, and the mean squared angular displacement $< \theta^2 >$ for rotational diffusion D_R by;

$$< z^2 >= 2D_T\Delta$$
$$< \theta^2 >= 4D_R\Delta$$

By considering theoretical models for friction factors (Figure S1), translational and rotational displacements due to diffusion over Δ can be calculated, as shown in figure S1. Unrestrained rotational diffusion applies in the limit $\Delta \to \infty$, which represents a regime where all rotations are equally likely. These displacements are plotted and compared in figure S2.

Geometry	f_T	f_R
Sphere	$6\pi\eta R$	$8\pi\eta R^3$
Rod	$3\pi\eta L \frac{1}{\ln(L/r)-0.3}$ [5]	$\frac{\pi\eta L^3}{3\ln\frac{L}{2r}}$ [6]

$$< z_{\text{rot}} >_{\text{restrained}} = \sqrt{\frac{2}{3}\left(1-\exp(-2D_R\Delta)\right)R^2}$$
$$< z_{\text{rot}} >_{\text{unrestrained}} = \sqrt{\frac{2}{3}R^2}$$
$$< z_{\text{trans}} > = \sqrt{2D_T\Delta} \tag{2}$$

Figure S1: Left - Translational and rotational friction factors for spheres of radius R, and rods of length L and radius r where η is the sample viscosity. Right - Equations for root mean squared displacements due to rotational and translational diffusion[7]. These are plotted in figure S2.

We note in this analysis that:

- A rod of length L will experience a greater translational rms displacement than a sphere of radius $R = L$.
- The rms displacement due to rotational diffusion becomes comparable to that of translation diffusion for rods of 1μm, and exceeds it for rods longer than 2μm.
- The rms displacement due to rotational diffusion becomes comparable to that of translational diffusion for spheres of radius 1μm, but never exceeds the rms displacement due to translational diffusion.

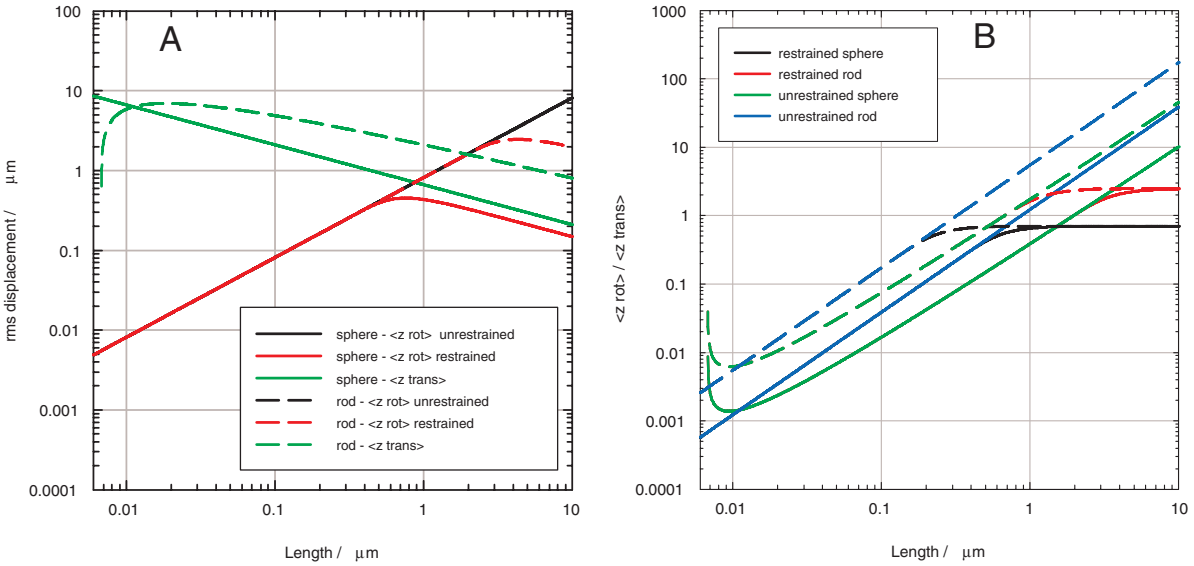

Figure S2: Plots of rms displacements due to rotational and translational diffusion for spheres and rods for $T = 300K$ and $\eta = 0.1cP$. A - rms displacement due to rotational and translational diffusion for rods and spheres, where $\Delta = 1s$. B - Ratio of rotational to translational diffusion for rods and spheres. Solid lines are for $\Delta = 1s$ and dashed lines are for $\Delta = 50ms$

- Decreasing Δ reduces the length where the rms displacement for translation becomes comparable to the rms displacement for rotation.

For rods, the limit $\lim_{L\to\infty} \frac{<z_{rot}>}{<z_{trans}>} = \sqrt{6}$ is reached where $L = 1\mu m$ for $\Delta = 100ms$ and by $L = 5\mu m$ for $\Delta = 1s$. For spheres, $\lim_{L\to\infty} \frac{<z_{rot}>}{<z_{trans}>} = \sqrt{\frac{1}{2}}$. This limit is reached for spheres of radius 200nm where $\Delta = 100ms$, and for spheres of radius $1\mu m$ where $\Delta = 1s$. In this limit, the formula for restricted rotational diffusion should be applied. Thus the relative contribution of rotational motion to the total rms displacement will be greater in general for a rod than a sphere. When the characteristic length is of the order 1μm, the magnitudes of both are comparable and rotational effects will then be manifested in the NMR diffusion experiment.

S4 - Rotational diffusion equations

The equations below describe the decay of PFGSE NMR resonances in cases where both Brownian rotational and translation motions are considered for single rods of length L and spheres of radius r, in the limit of unrestricted rotational diffusion[7].

$$\begin{array}{c|c} \text{Sphere} & S_i = S_0 \frac{\sin^2(\alpha r)}{\alpha^2 r^2} e^{-D_T \alpha^2 \Delta} \\ \text{Rods} & S_i = S_0 \frac{\cos(\alpha L) - 1 + \alpha L \int_{t=0}^{\alpha L} \frac{sin(t)}{t} dt}{\frac{1}{2}\alpha^2 L} e^{-D_T \alpha^2 \Delta} \end{array}$$

Models for D_T and D_R are those described in figure S1. The origin of the variance of D_{eff} with Δ is in the pre-exponential factor. Hence the gradient of the plot is given by the pre-exponential factor and does not depend on the model used for D_T. Empirically, the length distributions of amyloid fibrils measured using AFM/TEM take the form of log-normal distributions (Gaussian-like but skewed towards the greater probabilities of finding longer fibrils). The normalised log-normal distribution, defined as:

$$C(L) = \frac{1}{a_1\sqrt{2\pi}L} \exp\left[-\frac{(\ln(L/a_0))^2}{2a_1^2}\right] \tag{3}$$

The maximum of this distribution is given by $L_{max} = a_0 e^{-a_1^2}$, and the full width half maximum is $2\sinh(a_1\sqrt{\ln 4})L_{max}$. The modified equation to estimate the NMR signal from a species within a distribution for a given value of (G, δ, Δ) is given by:

$$\ln \frac{S_i}{S_0} = \frac{\sum_{L=0}^{\infty} C(L) S_i(L)}{\sum_{L=0}^{\infty} C(L) \lim_{G\to 0} S_i(L)} \tag{4}$$

With a model for D_T, the NMR signal intensity for a given a_1 and a_0 can be calculated. By comparing calculated NMR intensities with experimental data, we arrive at the fitted distributions shown in figure 2C in the main manuscript.

References

1. Baldwin, A. J., Bader, R., Christodoulou, J., MacPhee, C. E., Dobson, C. M., and Barker, P. D. *J. Am. Chem. Soc.* **128**(7), 2162–3 (2006).

2. Delaglio, F., Grzesiek, S., Vuister, G. W., Zhu, G., Pfeifer, J., and Bax, A. *J. Biol. NMR* **V6**(3), 277–293 (1995).

3. http://www.gnu.org/software/gsl/, (2007).

4. Rasband, W. *http//rsb.info.nih.gov/ij/* (1997).

5. Yamakawa, H. and Tanaka, G. *J. Chem. Phys.* **57**(4), 1537–1542 (1972).

6. Broersma, S. *J. Chem. Phys.* **32**(6), 1626–1631 (1960).

7. Baldwin, A., Christodoulou, J., Barker, P., Dobson, C., and Lippens, G. *J. Chem. Phys.* **127**(11), 114505 (2007).